



Correlated photofragment product distributions in the photodissociation of NO₂ at 212.8 nm

R.C. Richter, V.I. Khamaganov, A.J. Hynes *

Division of Marine and Atmospheric Chemistry, Rosenstiel School of Marine and Atmospheric Science, University of Miami, 4600 Rickenbacker Causeway, Miami, FL 33149, USA

Received 11 January 2000

Abstract

The 212.8 nm photolysis of NO₂ has been studied using REMPI–TOF and LIF techniques. Photodissociation occurs via a parallel transition on a time scale which is rapid compared to molecular rotation, producing anisotropic TOF profiles. Analysis of state selected NO flight profiles gives the correlated photofragment product distributions and shows that the predominant photodissociation channel produces vibrationally excited NO in $v = 3$ with O¹D as the co-fragment. If NO is formed in a rovibrational level for which O¹D production is energetically allowed then it is the exclusively produced co-fragment. © 2000 Elsevier Science B.V. All rights reserved.

1. Introduction

The photochemistry of NO₂ plays a critical role in the chemistry of the troposphere and stratosphere. Photodissociation in the first absorption band at wavelengths longer than 300 nm is the only in-situ source of ozone in the troposphere and in this wavelength region a single photodissociation channel, (1), is open producing both O and NO in their electronic ground states. Both the wavelength and temperature dependence of the photodissociation quantum yields and the detailed dynamics of the dissociation process have been the subject of extensive study. In recent work [1] it has been shown that sequential two-photon absorption provides a route to photolysis at wavelengths below the single-photon limit and that O¹D is a product of the photodissociation.

			Threshold
NO ₂ → O(³ P) +	NO(² Π)	(1)	398 nm
NO ₂ → O(¹ D) +	NO(² Π)	(2)	244 nm
NO ₂ → N(⁴ S) +	O ₂ (³ Σ ⁻)	(3)	275 nm

A second absorption feature extends from 250 nm into the vacuum ultraviolet and, in contrast to the first absorption feature, has not been the subject of extensive investigation. A steady state photolysis study by

* Corresponding author. Fax: +1-305-361-4689; e-mail: ahynes@rsmas.miami.edu

Preston and Cvetanovic [2] concluded that the quantum yield for O^1D production was 0.4 at 228.8 nm. Uselman and Lee [3] examined the wavelength dependence of the quantum yield, again using steady state photolysis techniques and obtained $\Phi_{O^1D} = 0.48$ at 228.8 nm and 0.41 at 213.9 nm. In a direct study Bigio et al. [4] photolyzed jet-cooled NO_2 , scanning a tunable laser between 220 and 226 nm. The single laser pulse was used to photolyze NO_2 and detect the NO photofragment via resonance enhanced multiphoton ionization (REMPI) on the A–X (0–0, 1–1, 2–2) transitions. Shafer et al. [5] studied O^1D production from the 205.47 nm photolysis of NO_2 , again a single laser was used to both photolyze NO_2 and detect the photofragment O^1D using REMPI. The only recent investigations are a presentation of these results [6] and a REMPI/ion imaging study of O^3P production in the 212.8 nm photolysis of jet-cooled NO_2 by Ahmed et al. [7]. In this work we have used 212.8 nm photolysis combined with REMPI–time of flight (TOF) and laser-induced fluorescence (LIF) techniques to study the energy disposal and yields of the correlated NO, O^1D and O^3P photofragments.

2. Experimental

Most of the experiments were performed in a time-of-flight mass spectrometer constructed in this laboratory and based on the design of Wiley and Maclaren. It consisted of an ionization chamber evacuated by a 4" diffusion pump connected to a flight tube evacuated by a 2" diffusion pump. Optical access to the ionization chamber was provided by two quartz windows which allowed a laser beam to propagate through the chamber, perpendicular to the axis of the flight tube, between the brass repeller and attractor plates which constitute the extraction region of the spectrometer. An effusive beam of NO_2 entered the ionization chamber and propagated perpendicular to the plane formed by the optical and spectrometer axes. TOF profiles of a thermal NO beam give a translational temperature of 300 K. In a typical experiment the photolysis and probe laser beams counterpropagated through the chamber intersecting the NO_2 beam. The delay between the lasers was controlled by a digital delay generator. Photoions were extracted into a 30 cm flight tube and detected by an MSP plate. The ion arrival signal was amplified and digitized using a 500 MHz oscilloscope. The 212.8 nm fifth harmonic of a Nd:YAG laser was used for photolysis. Probe laser pulses were generated using a frequency-doubled optical parametric oscillator pumped by the 3rd harmonic of a Nd:YAG laser. Both lasers were linearly polarized and the angle between their planes of polarization and the spectrometer axis could be varied continuously using half-wave plates. Since the flight tube is horizontal, a horizontally polarized beam has its axis of polarization parallel to the flight tube axis. The NO product was detected by (1 + 1) REMPI on the A–X transition. O^3P was detected by (2 + 1) REMPI on the $3p^3P - 2p^3P_{2,1,0}$ transitions at 226 nm. Attempts to directly detect O^1D using (3 + 1) REMPI at 276 nm [8] were unsuccessful with the signal being dominated by multiphoton production of O^1D by the focused probe laser. A set of experiments to determine the relative yields of $O^3P:O^1D$ was performed in a glass cell evacuated by a rotary pump. Two-photon LIF was used to monitor the appearance of O^3P after the 212.8 nm photolysis. The $3p^3P - 2p^3P_{2,1,0}$ transitions were used for excitation with fluorescence monitored on the $3p^3P_{2,1,0} - 3s^3S_1$ transition at 845 nm. Temporal profiles of O^3P were obtained by monitoring the two-photon LIF signal as a function of the delay time between the lasers.

3. Results

3.1. REMPI–TOF experiments

In this experiment photolysis by a polarized laser at 212.8 nm produces photofragments which are then ionized by a probe laser and detected after passage through a time-of-flight mass spectrometer. Measurement of the ion current as a function of probe laser wavelength gives the REMPI spectrum shown in Fig. 1a. The spectrum shows the $A^2\Sigma^+ - X^2\Pi$ (1–3) and (0–2) bands and clearly identifies the production of vibrationally

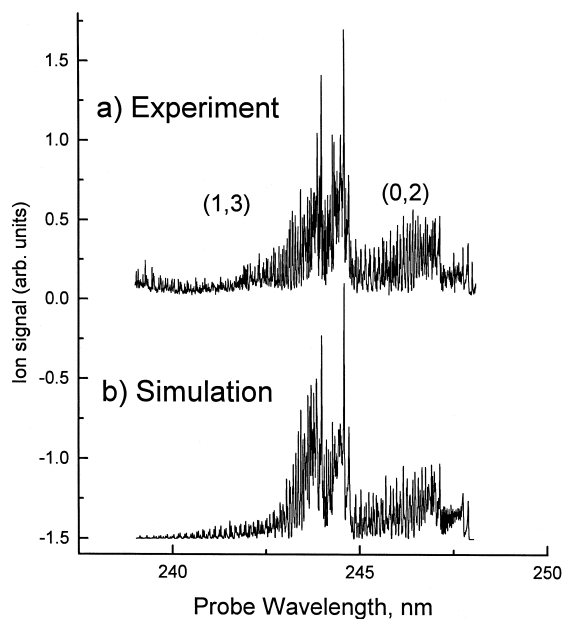


Fig. 1. (a) REMPI spectrum of the $A^2\Sigma^+ - X^2\Pi$ (1–3) and (0–2) bands of NO produced by the 212.8 nm photolysis of NO. (b) Simulation of the excitation spectrum.

excited NO. Fig. 1b shows a spectral simulation obtained using the program LIFBASE [9]. By fixing the probe laser on a particular rovibrational transition and monitoring the ion current as a function of time we obtain a TOF profile for that fragment. Figs. 2 and 3 show TOF profiles of NO photofragments. In Fig. 2 ionization occurs via excitation of the overlapping $Q_1(21)$, $Q_{21}(21)$ and $R_2(20)$ lines of the A–X (0–2) band. Hence we detect NO fragments with $v = 2$ and $J = 21.5$ from the $^2\Pi_{1/2}$ spin–orbit component and $J = 19.5$ from the $^2\Pi_{3/2}$. The shape of the observed profiles can be interpreted as follows. Richie and Walsh [10] have analyzed the rotational structure of NO_2 bands at 2491 Å and concluded that the transition is $^2B_2 - ^2A_1$, a parallel transition in which the transition dipole lies in the plane of the molecule. If absorption at 212.8 nm occurs via

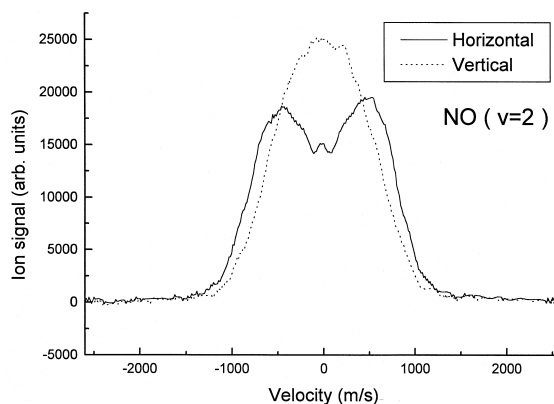


Fig. 2. Time-of-flight profiles of state selected NO $v = 2$, $J = 21.5$, 19.5 fragments produced by the 212.8 nm photolysis of NO_2 . Solid line obtained with horizontally polarized photolysis laser, dotted line obtained with vertical polarization.

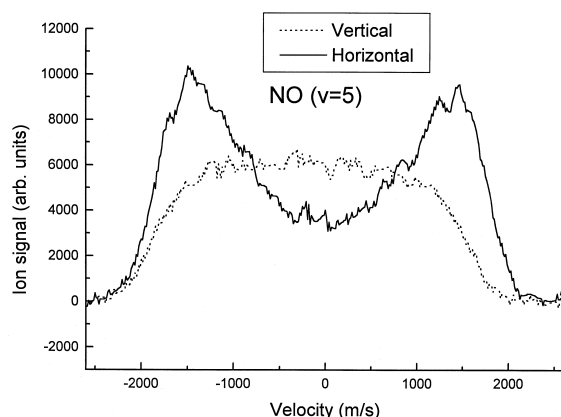


Fig. 3. Time-of-flight profiles of state selected NO $v = 5$, $J = 42.5$, 36.5 fragments produced by the 212.8 nm photolysis of NO_2 . Solid line obtained with horizontally polarized photolysis laser, dotted line obtained with vertical polarization.

the same transition then excitation with horizontally polarized light excites those molecules with their transition dipoles aligned parallel to the axis of the flight tube. If dissociation takes place on a timescale which is short compared with a rotational period then the fragments recoil along the axis of the flight tube in forward and backward directions. The arrival time profile of the ionized fragments at the detector reflects the initial velocity distribution of the state selected neutral photofragments. The ions which recoil away from the detector have their direction reversed by the field and arrive at the detector after the ions which recoil forwards towards the detector. The time between the arrival of the peaks depends on the recoil velocity of the parent neutral photofragments, the larger the velocity the longer the time. Hence in Fig. 2, the profile obtained with horizontally polarized photolysis shows two peaks corresponding to fragment velocities of ~ 500 m/s and consistent with a parallel transition. The TOF profile with vertically polarized photolysis has a single peak. In this case the photofragments recoil perpendicular to the spectrometer axis. The observed velocity profile can be rationalized in terms of the energetics of the photodissociation which are summarized in Table 1. NO fragments produced in $v = 2$, $J = 19.5$, 21.5 could be produced by either reaction (1) or reaction (2). If the fragments are formed via reaction (1) more than $17\,000\text{ cm}^{-1}$ of energy is disposed into translation producing NO fragments with a velocity of ~ 2200 m/s. However, if the fragments are produced via reaction (2), less than 2000 cm^{-1}

Table 1

Energetics of photofragment production at 246.214 nm

Excitation: 246.214 nm, Fig. 2b), A–X (0–2), $Q_1(21)$, $Q_{21}(21)$, $R_2(20)$. Branch: $Q_1(21)$, $Q_{21}(21)$, $J = 21.5$ $R_2(20)$, $J = 19.5$

Reaction (1), $\text{NO} + \text{O}^3\text{P}$

J	Available energy (cm^{-1})	NO velocity (m/s)	O^3P velocity (m/s)
19.5	17477	2201	4128
21.5	17200	2184	4096

Reaction (2), $\text{NO} + \text{O}^1\text{D}$

J	Available energy (cm^{-1})	NO velocity (m/s)	O^1D velocity (m/s)
19.5	1337	609	1142
21.5	1614	669	1254

is available for translation and the NO fragments are produced with velocities of 610 and 670 m/s. The TOF profile, Fig. 2, shows that no fast NO fragments are formed and that NO production occurs exclusively via reaction (2) with O¹D as the co-fragment.

In contrast, Fig. 3 shows the TOF profiles obtained by excitation of overlapping lines in the A–X (2–5) band at 247.995 nm. In this case we excite the overlapping Q₂(43) and R₁(36) transitions probing fragments in both spin–orbit components in $v = 5$, $J = 42.5, 36.5$. The photodissociation energetics are summarized in Table 2. In this case production of O¹D is not energetically feasible and only reaction (1) is open, predicting NO fragment velocities of ~ 1700 m/s with O³P as the co-fragment. The observed TOF profiles are consistent with this and again indicate an anisotropic dissociation via a parallel transition. We obtained TOF profiles for NO fragments produced in vibrational levels $v = 0–5$. In some cases analysis is complicated by simultaneous excitation of multiple levels, however the results are consistent with O¹D being the exclusive co-fragment produced with NO $v = 0, 1, 2, 3$. For NO $v = 4, 5$ O³P is the only energetically allowed co-fragment.

We attempted to directly monitor O¹D via (3 + 1) REMPI at ~ 276 nm, however in this case production of O¹D via multiphoton dissociation by the tightly focused probe laser dominated over production via the 212.8 nm photolysis. O³P was detected via excitation of the $3p^3P - 2p^3P_{2,1,0}$ transitions at 226 nm. Strong ‘probe only’ signals were observed at the excitation wavelength of each spin–orbit component. Fig. 4 shows TOF profiles for O³P₂ obtained after photolysis with the horizontally and vertically polarized 212.8 nm laser and after subtraction of the probe signal. In this case the coproduced NO fragments can be formed in any of the 12 energetically accessible vibrational energy levels and hence the O³P₂ can be formed with velocities ranging from 0 to almost 5000 m/s. In contrast to the TOF profiles of the NO fragments shown in Figs. 2 and 3 which have well-defined translational energies, Fig. 4 is a superimposition of many such profiles and consequently is rather more difficult to interpret. The energy scale in the figure shows the O³P₂ fragment velocities corresponding to the production of NO in a specific vibrational level. It is immediately clear that there is no production of fast O³P₂ atoms which would correspond to co-fragment NO molecules produced in the first four vibrational levels. Our TOF profiles of NO fragments produced in $v = 4, 5$ are indicative of anisotropic dissociation, clearly the coproduced O³P₂ has an identical anisotropy. If this holds for all O³P₂ production then the lack of a clearly defined anisotropic profile in Fig. 4 indicates that O³P₂ must be formed with a significant fast and slow components. A more detailed analysis would require a simulation of the superimposed profiles and would require a knowledge of the NO vibrational state distribution in $v = 5–12$. For O³P₁ we found a significant signal due to the probe laser but very little signal due to 212.8 nm photolysis, a direct comparison of the respective ion signals at similar photolysis powers gives an O³P₂:O³P₁ ratio of $\sim 11:1$. For O³P₀, variation in photolysis and probe power precluded determining a ratio of the signals but again suggested that the signal is much smaller than that obtained for O³P₂.

The relative importance of channels (1) and (2) can be assessed from yields of the photofragments, both from an analysis of the vibrational product distribution of the NO fragments and by directly measuring the relative yields of O¹D and O³P. REMPI excitation spectra were obtained by scanning the probe laser between 220 and

Table 2

Energetics of photofragment production at 246.214 nm

Excitation: 247.995 nm, Fig. 2a), A–X (2–5), Q₂(43), Q₁₂(43), R₁(36), P₂₁(36). Branch: Q₂(43), Q₁₂(43), $J = 42.5$, R₁(36), P₂₁(36), $J = 36.5$ Reaction (1), NO + O³P

J	Available energy (cm ⁻¹)	NO velocity (m/s)	O ³ P velocity (m/s)
36.5	10421	1700	3187
42.5	9831	1651	3096

Reaction (2), NO + O¹D: endothermic

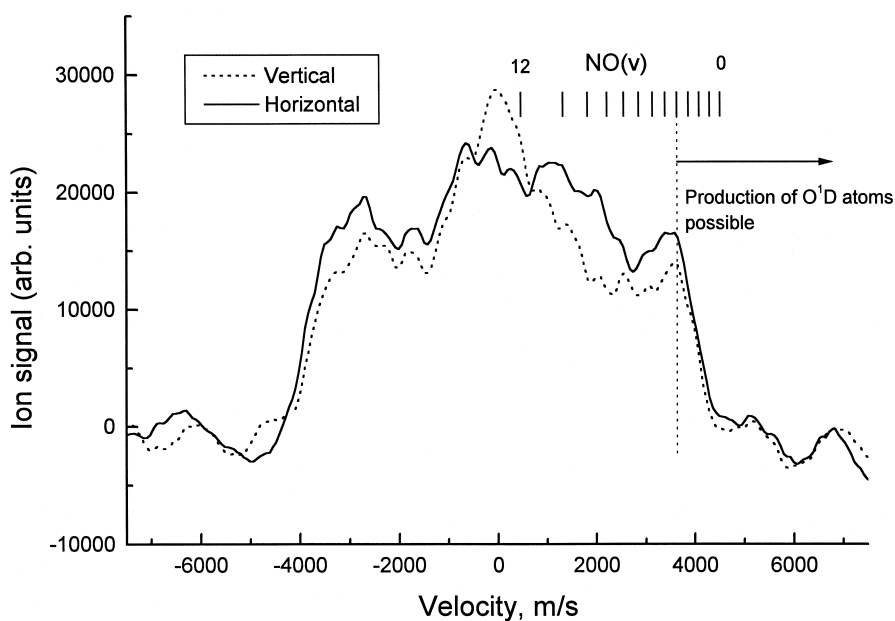


Fig. 4. Time-of-flight profiles of O^3P_2 produced by the 212.8 nm photolysis of NO. Solid line obtained with horizontally polarized photolysis laser, dotted line obtained with vertical polarization.

250 nm. Spectra were analyzed using the LIFBASE program assuming that the REMPI spectra can be described by the single-photon A–X transition probabilities. The simulated spectrum shown in Fig. 1b is based on NO formation with an inverted vibrational population distribution peaking in $v = 3$, and with a $v = 3:2$ ratio of 4:1. The simulation requires a large population for levels that can be coproduced with O^1D and little population in the levels which are energetically restricted to O^3P as the co-fragment. The signal levels at the (0–0), (1–1), and (2–2) bands were adequate to obtain TOF profiles but were noisier and of lower quality than the (1–3) and (0–2) bands, due in part to a significant ‘probe only’ signal. Based on the observed signal levels we estimate that population in $v = 0$ and 1 is less than $v = 2$ but LIF would clearly be a better approach to the extraction of these populations. Extraction of population distributions from REMPI signals has potential complications and direct observation of all the vibrational product yields using LIF would complement this analysis.

3.2. Kinetics

In order to attempt to directly determine the $O^1D:O^3P$ yields we monitored the temporal profiles of O^3P production after photolysis of NO_2 in N_2 or He buffer. Fig. 5 shows the risetime in the O^3P_2 signal after photolysis of an 0.2% mixture of NO_2 in N_2 at ~ 8 Torr total pressure. Under these conditions the main fate of the photolytically produced O^1D should be collisional relaxation to O^3P . O^3P was monitored by two-photon LIF. By comparing the ‘prompt’ O^3P production to the O^3P produced by relaxation the relative yields of $O^1D:O^3P$ can be determined. The points at $t < 0$ show the signal prior to the laser photolysis after subtraction of the ‘probe-only LIF’ which was $\sim 25\%$ of the peak signal. The data were fit to an exponential rise-and-fall expression:

$$[O^3P]_t = [O^3P]_0 + [O^1D]_0(1 - \exp(-k_q[N_2]t))\exp - k_1t,$$

where $[O^3P]_0$, $[O^1D]_0$ are the initial concentrations of O^3P and O^1D ; k_q is the quenching rate coefficient of O^1D by N_2 and k_1 is the background loss rate of O^3P .

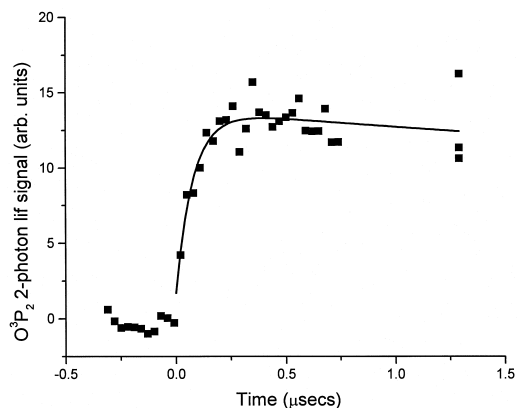


Fig. 5. Temporal profile of O^3P_2 produced by the 212.8 nm photolysis of NO. The solid line shows the best fit to an "exponential rise and fall". Fit parameters are given in the text.

The solid line shows the fit curve which gives relative yields of $O^3P:O^1D$ of $(1.7 \pm 2.1):(12.1 \pm 2.0)$, i.e. a ratio of 1:7 or 87.5% of the O atoms are produced as O^1D . The error bars are such that the data would be consistent with an O^1D yield between 1 and 0.7. The quenching rate is $(1.2 \pm 0.2) \times 10^7 \text{ s}^{-1}$. This is a factor of 2 larger than the rate calculated using the recommended quenching rate, $2.6 \times 10^{-11} \text{ cm}^3 \text{ molecule}^{-1} \text{ s}^{-1}$. A similar experiment in a 1% mixture of NO_2 in He buffer gave similar results including a very fast quenching rate. However, He is not an efficient quencher of O^1D . Temporal profiles of O^3P_1 and O^3P_0 gave scattered plots which were impossible to interpret. This may be due to the competition between production and relaxation to O^3P_2 . The O^3P_2 results are consistent with reaction (2) being the predominant production channel but further experiments are needed to understand these profiles and better quantify the O^1D yield.

In summary, our results indicate that excitation of NO_2 at 212.8 nm occurs via a parallel transition. Photodissociation occurs on a time scale which is rapid compared to molecular rotation producing anisotropic TOF profiles. Our results suggest that photodissociation occurs predominantly via channel (2) producing O^1D and NO with a vibrational population distribution which peaks in $v = 3$. Channel (1) produces O^3P and NO in vibrational levels ≥ 4 . If NO is formed in a rovibrational level for which O^1D is an energetically allowed co-fragment then it is the exclusively produced co-fragment even though production of O^3P would be both spin and energetically allowed. The only production of O^3P occurs as a channel producing highly vibrationally excited NO as the co-fragment. These results suggest that 212.8 nm photolysis of NO_2 is a good source of O^1D for both kinetics and dynamics studies.

Acknowledgements

This work was supported by the National Science Foundation through grant ATM-9625437 and the Office of Naval Research through DURIP grant No. N000149710480. We thank Dr. J. Luque, and Dr. D.R. Crosley for providing a copy of LIFBASE.

References

- [1] J.N. Crowley, S.N. Carl, *J. Phys. Chem.* 101 (1997) 4178.
- [2] K.F. Preston, R.J. Cvetanovic, *J. Chem. Phys.* 45 (1966) 2888.
- [3] W.M. Uselman, E.K.C. Lee, *J. Chem. Phys.* 65 (1976) 1948.

- [4] L. Bigio, R.S. Tapper, E.R. Grant, *J. Phys. Chem.* 88 (1984) 1271.
- [5] N. Shafer, K. Tonokura, Y. Matsumi, S. Tasaki, M. Kawasaki, *J. Chem. Phys.* 95 (1991) 6218.
- [6] R.C. Richter, V.I. Khamaganov, A.J. Hynes, 15th Int. Symp. on Gas Kinetics, Bilbao, Sept. 1998, Pap. D54.
- [7] M. Ahmed, D. Peterka, A.S. Bracker, O.S. Vasyutinski, A.G. Suits, *J. Chem. Phys.* 110 (1999) 4115.
- [8] R.C. Richter, A.J. Hynes, *J. Phys. Chem.* 100 (1996) 8061.
- [9] J. Luque, D.R. Crosley, LIFBASE: Database and Spectral Simulation Program (Version 1.45), SRI International, Pasadena, CA, Rep. MP 98-021.
- [10] R.W. Richie, A.D. Walsh, *Proc. R. Soc. London, Ser. A* 267 (1962) 395.